Turbulence Determination and Blockage Correction for Immersed Cylinder Heat Transfer at High Reynolds Numbers

ELIYAHU TALMOR

Rocketdyne, Canoga Park, California

Transitional immersed cylinder heat transfer measurements are used in conjunction with the theory of boundary-layer transition of van Driest and Blumer to determine the corresponding free-stream turbulence intensity. The consistency of the results is demonstrated by comparison to other investigations where the free-stream turbulence intensity was directly measured with a favorable pressure gradient present. Successful determination of the turbulence level for high blockage data and proper correction for channel blockage effects for all data compared lead to an improved and extended correlation of immersed cylinder average and stagnation point heat transfer results. Concurrently, a boundary-layer transition theory is extended from zero pressure gradient and moderate turbulence levels to conditions of high turbulence and high pressure gradient.

Turbulence intensity is generally measured by hot wires, gas sampling (via gas phase mixing), and optical techniques (*1*). However, high-temperature conditions (*2* to *4*) associated with combustion eliminate the hot wire and gas sampling methods, leaving optical methods for consideration. These methods require the employment of an optical tracer in conjunction with an assumed turbulent diffusion model for data interpretation (*1*). Although they have merit, these techniques constitute one example of indirect methods for measuring free-stream turbulence intensity in high-temperature gas streams. Another indirect method could be realized through heat transfer measurements obtained with combustion-induced turbulence present. In a way, the employment of heat transfer measurements for determining combustion-induced turbulence intensities is more of a direct method than the optical ones, as it does not involve a foreign tracer, the injection of which has an unknown effect on the turbulence to be measured.

The effect of turbulence level on convective heat and mass transfer from immersed cylinders is well known (*5* to *10*). Both the average heat transfer rate (*6*) and the local heat transfer rate (*9*) were found to increase with the free-stream turbulence intensity.

Generally, the effect of free-stream turbulence on immersed cylinder heat transfer has been found to be analogous to the effect of sound on heat transfer (*11*). In particular, the stagnation region appears to be most sensitive to free-stream turbulence effects (*7, 8, 12, 13*).

Heat transfer results for immersed cylinders in a high-temperature transonic cross flow have just recently been reported (*2, 3*). Two such investigations, with combustion-induced turbulence present, indicate that the boundary layer around small- (*3*) and large- (*2*) diameter throat tubes is turbulent essentially from the stagnation point. Actually, since local heat transfer measurements were taken at 20-deg. intervals (*2*) and since the boundary layer was found to be turbulent 20 deg. away from the stagnation point, the latest the transition point can be postulated to exist is approximately 10 deg. away from the stagnation point. While a successful correlation of the data was developed (*3, 4*), the results could not be compared to those obtained by others at subsonic speeds and screen-induced turbulence levels, because the turbulence intensity of the high-temperature experiments could not be measured.

It is the purpose of this paper to provide such a comparison among widely ranged immersed cylinder heat transfer data by first determining the combustion-induced turbulence intensity from its corresponding heat transfer data (*2, 3*) and second, by properly correcting for channel blockage effects for all data compared (*2, 3, 6, 8, 9, 14* to *16*). In attaining this objective, two other accomplishments are made: A boundary-layer transition theory (*17*) is extended from flat plate moderate turbulence levels to conditions of high turbulence and high pressure gradient, and a new tool is provided for determining turbulence intensities in high-temperature combustors.

DETERMINATION OF COMBUSTION-INDUCED TURBULENCE INTENSITY

Pertinent heat transfer data (*3*) for ⅜-in. O.D. cylinders at a channel blockage ratio (D/W) of 0.75 are given in Figure 1 in the form of log average heat transfer co-

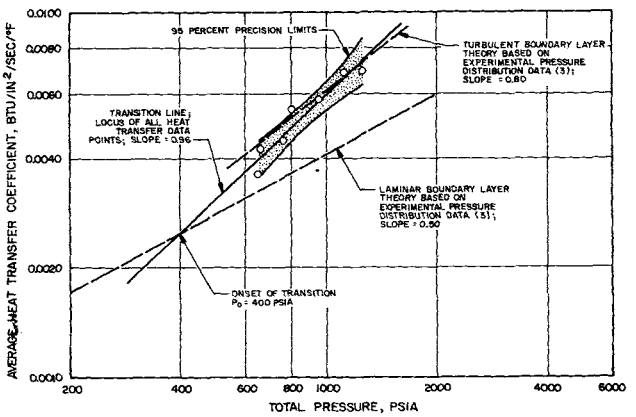

Fig. 1. Transitional heat transfer averages (3) for an immersed ⅜-in. O.D. cylinder at a channel blockage ratio of 0.750. $239{,}000 < (N_{Re})_{D,T_{t_\infty}} < 447{,}000$.

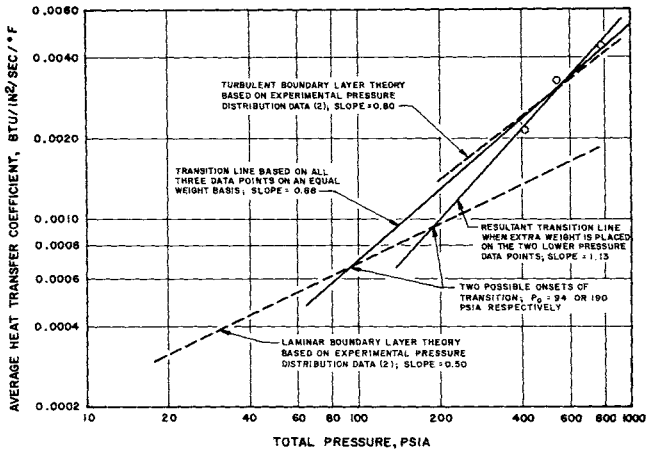

Fig. 2. Transitional heat transfer averages (2) for an immersed 1.25-in. O.D. cylinder at a channel blockage ratio of 0.667. 583,000< $(N_{Re})_{D,r_\infty}$ <1,000,000.

efficients vs. log total pressure, which is analogous (in this case) to plotting log Nusselt number vs. log Reynolds number. The lower and upper dotted lines represent laminar and turbulent heat transfer levels as derived from corresponding experimental pressure distribution data (3), while the data points in Figure 1 represent actual heat transfer measurements obtained by water calorimetry. The solidly drawn transition line is the best straight line fit of the data and it indicates the onset of transition to occur at a total pressure of 400 lb./sq.in.abs. with transition ending at a total pressure of 1,250 lb./sq.in.abs. The location of the 95% precision band of the data with respect to the turbulent line indeed justifies the inclusion of all data points for generating the transition line, thus implying that all the heat transfer points involved are in a transitional boundary-layer flow regime.

A similar presentation of heat transfer data (2) for a 1.25-in. O.D. cylinder at a channel blockage ratio of 0.667 is given in Figure 2. However, only three data points (derived from transient temperature measurements) are available in this case. Therefore, no precision limits are shown. Nevertheless, it is noted that the 410 lb./sq.in.abs. data point is clearly in the transition zone and the 780 lb./sq.in.abs. point is clearly in a turbulent boundary-layer flow regime leaving an uncertainty regarding the intermediate point at 540 lb./sq.in.abs. Therefore, two possible transition lines are shown in Figure 2. One transition line is a straight line fit of all three data points on an equal weight basis (2), indicating that the transition regime exists between total pressures of 94 and 500 lb./sq.in.abs. The other transition line (190 to 550 lb./sq.in.abs.) results when extra weight is placed on the two lower pressure data points (410 and 540 lb./sq.in.abs.). Both transition lines will be considered in the treatment to follow. The boundary-layer transition data given in Figures 1 and 2 in conjunction with their corresponding pressure distribution data (2, 3) will be used to determine the turbulence intensity involved by application of a theory of boundary-layer transition (17) which includes effects of free-stream turbulence and pressure gradient.

Van Driest and Blumer (17) formulated a suitable transition criterion by assuming that the breakdown of laminar flow occurs when the local shear within the boundary layer is sufficiently remote from the surface, that is, when the vorticity Reynolds number (ratio of local inertial stress to local viscous stress) reaches a maximum value. With this assumption, the method of Taylor is followed for introducing turbulence into the flow and the laminar boundary-layer solution of Falkner-Skan is used to account for the effect of pressure gradient on transition. The resulting transition equation is given (17) as

$$\frac{1{,}690}{(N_{Re})_{x,e,t}} = \frac{0.312}{(m+0.11)^{0.528}} + 0.73\eta_e^2\left(\frac{Tr}{100}\right)^2 (N_{Re})_{x,e,t}^{1/2} \qquad (1)$$

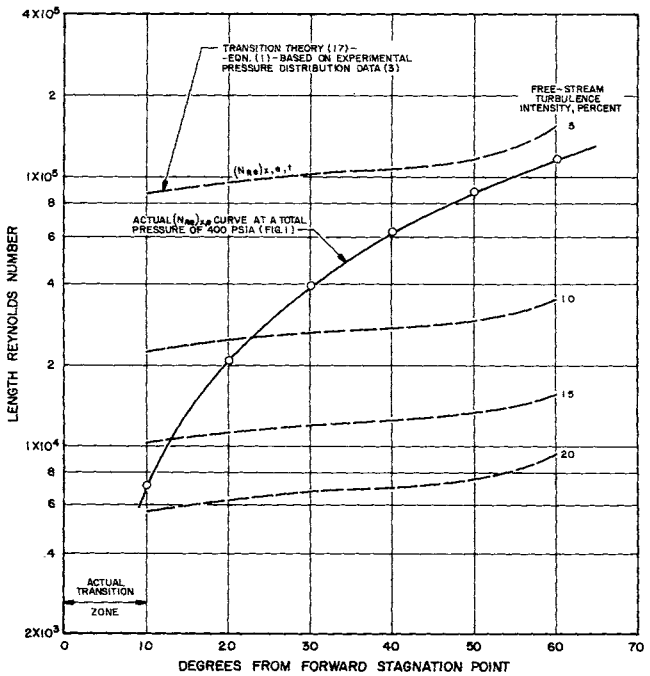

Fig. 3. Transition on a ⅜-in. O.D. cylinder (3) at a channel blockage ratio of 0.750 with combustion-induced turbulence present.

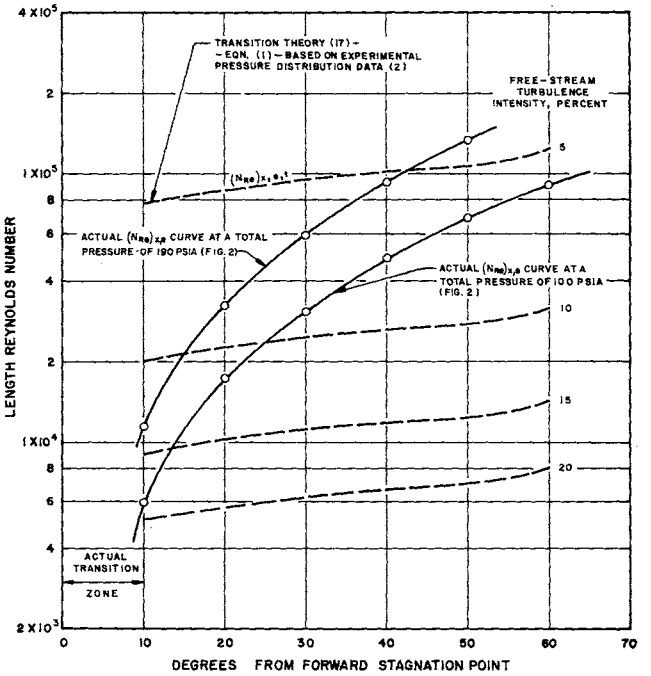

Fig. 4. Transition on a 1.25-in. O.D. cylinder (2) at a channel blockage ratio of 0.667 with combustion-induced turbulence present.

where the first term on the right-hand side of this equation is a strict pressure gradient term and the second term is a function of both free-stream turbulence intensity and pressure gradient (η_e is a unique function of m). Equation (1) fits flat plate ($m = 0$) transition data well. In fact, some of the constants involved were determined from flat plate, zero pressure gradient transition data (*17*).

In order to apply Equation (1) to the extreme pressure gradient conditions of the data of Figures 1 and 2, corresponding local values of m have to be known. These were determined from corresponding experimental pressure distribution data (*2, 3*) by writing Euler's equation along the outer edge of the boundary layer. Local velocities were then plotted vs. distance from stagnation (or angle from stagnation) on log-log coordinates and local slopes m taken ($u_e \sim x^m$). With the local m's known, Equation (1) yields $(N_{Re})_{x,e,t}$ vs. degrees from stagnation at given values of Tr as shown by the dotted curves in Figures 3 and 4 for the small (*3*) and large (*2*) cylinders, respectively.

For the 3/8-in. O.D. cylinder at a channel blockage ratio of 0.75, the onset of transition occurs at a total pressure of 400 lb./sq.in.abs. (Figure 1). Therefore, the actual local length Reynolds number curve at 400 lb./sq.in.abs. is superimposed on Figure 3 for comparison. As shown, to obtain transition at 400 lb./sq.in.abs. in the range of 0 to 10 deg. from forward stagnation the turbulence intensity has to be at least 20% [$(N_{Re})_{x,e,t} = 5{,}700$].

Similar actual local length Reynolds number curves at total pressure of 94 and 190 lb./sq.in.abs. are given in Figure 4 for the 1.25-in. O.D. cylinder at a channel blockage ratio of 0.667. The two curves reflect the two possible transition lines of Figure 2. As shown, transition at $p_o =$ 94 lb./sq.in.abs. in the range of 0 to 10 deg. from forward stagnation requires a turbulence intensity of at least 20% [$(N_{Re})_{x,e,t} = 5{,}100$], while a similar transition at $p_o = 190$ lb./sq.in.abs. requires a free-stream turbulence intensity of at least 15% [$(N_{Re})_{x,e,t} = 9{,}000$]. The lower value of turbulence intensity for the large cylinder seems more realistic since the large cylinder was placed 23 in. from the main propellants injector (*3*), while the small cylinders were placed 6 in. from the injector (*2*). Combustion-induced free-stream turbulence is known to decay with distance from the main propellants injector (*1*).

It should be noted that the apparent need for a choice between two possible turbulence levels is not a shortcoming of the method used to determine the turbulence intensity involved but rather the result of having a limited number of heat transfer data points (Figure 2).

The consistency of the transition and turbulence results derived herein can be demonstrated by comparison to other investigations where the free-stream turbulence intensity was directly measured with a favorable pressure gradient present. Such a comparison is graphically presented in Figure 5 where the data of this paper are shown to correlate markedly well with those of Buyuktur et al. (*18*) and of Thomas (*19*). The lower curve represents the start of transition (last point on the laminar line) and the upper one represents the end of transition (first point on the turbulent line). All the transition data of Figure 5, derived from mass and heat transfer measurements, are in good agreement with the extrapolated flat plate zero pressure gradient curves of Gazley (*19, 20*).

The reported combustion-induced turbulence intensity values are approximate in the sense that the exact location of the transition point within the range of 0 to 10 deg. from stagnation is not known. Nevertheless, knowing that the turbulence intensity is at least 20% for the small cylinders study (*3*) and at least 15% for large cylinder investigation (*2*) is of utmost significance for a comparison of these heat transfer results (*2, 3*) with those ob-

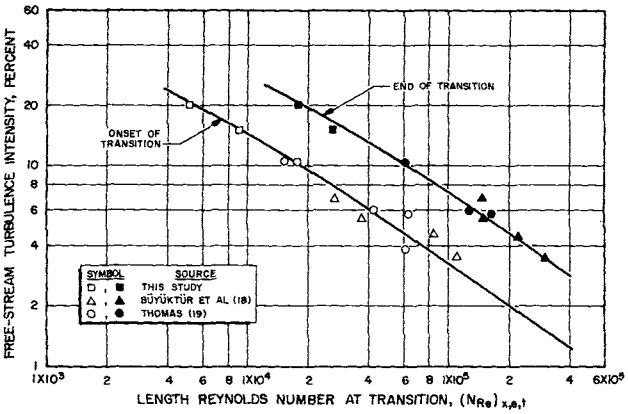

Fig. 5. Effect of free-stream turbulence intensity on boundary-layer transition.

tained by others at lower screen-induced free-stream turbulence intensities. However, such a comparison cannot be made without proper correction for channel blockage effects.

CORRECTION FOR CHANNEL BLOCKAGE

Channel blockage influences heat transfer through its effect on the velocity distribution around the immersed cylinder. Two methods of blockage corrections have generally been employed: correction of the Nusselt number and correction of the Reynolds number (*13*). The latter seems more appropriate, since blockage affects velocity in a more direct manner.

Perkins and Leppert (*13*) determined an empirical correction factor for the Reynolds number which combines the Nusselt numbers at various blockage ratios into a single curve when plotted vs. the corrected Reynolds numbers. The average of their local corrections for the average Nusselt number around the immersed cylinder was found to be in good agreement with the velocity correction suggested by Pope (*22*), that is

$$u^* = u_\infty [1 + 0.822\,(D/W)^2 + (C_D/4)\,(D/W)] \quad (2)$$

where the second term corrects for solid blocking and the third term corrects for wake blocking. Equation (2) was derived by Pope (*22*), who used the potential flow theory and the method of images. It will be employed here for blockage correction of Reynolds numbers of various investigations (*2, 3, 6, 9, 14* to *16*).

Knudsen and Katz (*23*) suggest the correction of $(N_{Nu})_{D,r,\text{avg.}}$ by a factor of $\sqrt{1 + (D/W)}$ to consider the effect of blockage on average heat transfer on circular cylinders. However, this factor has no experimental verification.

A blockage correction factor for the forward stagnation point heat transfer is given by Robinson and Han (*21*). They determined an empirical correction factor $(1 + \sqrt{D/W})$ for the Reynolds number which yields an agreement between their stagnation point heat transfer data at various blockage ratios ($0.25 < D/W < 0.75$) and the theoretical prediction of Squire (*24*) for a cylinder in free stream (zero blockage). The blockage correction factor of Robinson and Han (*21*) will be used to compare stagnation point heat transfer results of various investigations (*2, 3, 8, 9, 14, 15*).

CORRECTION FOR HIGH TEMPERATURE-DIFFERENCE

Douglas and Churchill (*25*) reanalyzed available data for convective heat transfer between gases and immersed cylinders with moderate and low-temperature differences.

They obtained a better correlation of the average heat transfer data when the thermal conductivity and kinematic viscosity of the gas are evaluated at the arithmetic average of free-stream and surface temperatures, that is, $0.5(T_w + T_e)$. Their recommendation as to the film properties will be generally followed for the extreme temperature difference conditions of Figures 1 and 2, except that the reference temperature will be taken as the arithmetic average of the adiabatic wall temperature and the actual wall temperature (3), that is, $0.5(T_w + T_{aw})$. With the Prandtl number being close to unity (2, 3, 16), the adiabatic wall temperature is very close to the gas stagnation temperature (T_o).

RESULTS AND DISCUSSION

A correlation of extended immersed cylinder heat transfer data is graphically presented in Figure 6 in the form of $(N_{Nu})_{D,r,\text{avg.}}/(N_{Pr})^{1/3}$ vs. $K_{\text{avg.}}\,(N_{Re})_{D,r,\infty}$ where $K_{\text{avg.}} = 1 + 0.822\,(D/W)^2 + (C_D/4)(D/W)$. The marked consistency of the various sets of data is rather striking. The zero blockage and zero turbulence data of Schmidt and Wenner (14), the 0.9% turbulence intensity data ($D/W = 0.108$) of Zapp (9), the 0.63 to 0.87% turbulence intensity data ($D/W = 0.19$) of Kestin and Maeder (6), and two of the data points of Giedt (15) are all well correlated by the single lower curve labeled *0-1 percent turbulence intensity*. The 3% turbulence curve drawn through corresponding data points of Zapp (9) shows good agreement with respect to the 2.38 to 2.67% turbulence data of Kestin and Maeder (6). Furthermore, it reveals that four of the data points of Giedt (15), reported to have been obtained at zero turbulence, apparently correspond to a turbulence level on the order of 3%.

All the data points represented by the three lower curves on the left-hand side of Figure 6 correspond to immersed cylinder boundary layers that are either completely laminar or partially laminar and partially turbulent. The results for essentially turbulent boundary layers (2, 3) are shown on the right-hand side of Figure 6. These are the data points of Figures 1 and 2 obtained at channel blockage ratios of 0.750 and 0.667 and combustion-induced turbulence intensities of at least 20 and 15%, respectively. The upper straight line on the right-hand side of Figure 6 represents the semianalytical turbulent heat transfer correlation (3) of the data corresponding to the equation

$$\frac{(N_{Nu})_{D,o,s \text{ or avg.}}}{(N_{Pr})^{1/3}} \left[\frac{(N_{Ma})_\infty}{(N_{Re})_{D,o,\infty}}\right]^{0.40} \left(\frac{\mu_o^2}{g_c\,\rho_o\,D^2 p_o}\right)^{0.20} \left(\frac{T_r}{T_o}\right)^{0.32} = 0.0155 \qquad (3)$$

where

$$\frac{T_r}{T_o} = 0.50\left(1 + \frac{T_w}{T_o}\right)$$

The constant on the right-hand side of Equation (3) was revised from its original value (3) of 0.0145, reflecting the fact that the lower total pressure data points in Figures 1 and 2 are clearly in a transitional boundary-layer flow regime and therefore should not be used to determine a constant in a turbulent heat transfer equation.

The original constant was based on all data points, transitional and turbulent. To clarify further the identity of the two data categories, the 20 and 15% turbulence intensity transition lines in accordance with Figure 5 are shown dotted in Figure 6. Both lines correlate data points falling between the turbulent and the 0 to 1% turbulence-intensity heat transfer levels.

Of particular interest are the calorimetric heat transfer results of Nelson and Talmor (16) obtained with a 0.60-

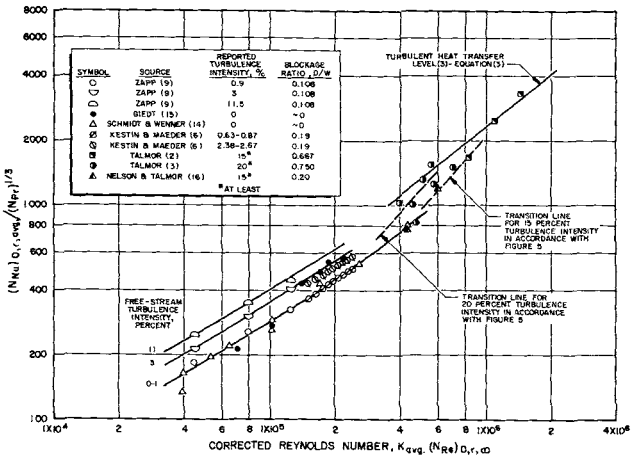

Fig. 6. Correlation of immersed cylinder average heat transfer coefficients at high Reynolds numbers and a wide range of blockage ratios and turbulence intensities.

in. O.D., 0.009-in. wall Inconel-X cylinder immersed in the subsonic converging section of a rocket combustion chamber generating the same high-temperature gas stream used for the throat-tube heat transfer investigations (Figures 1 and 2). Two data points were obtained at total pressures of 1,045 and 1,505 lb./sq.in.abs. The channel blockage ratio was 0.20, almost identical to that of Kestin and Maeder (6). While no pressure distribution data were taken for application of Equation (1), Figure 6 shows that the two heat transfer points follow the transition line corresponding to a turbulence intensity of 15%. This turbulence intensity is somewhat lower than that for the sonic cylinders (3) placed a short distance downstream of the subsonic cylinder, indicating that the free-stream turbulence intensity, while decaying with distance from the injector in the combustion zone (1), apparently increases with distance along the convergence zone where the gas stream is highly accelerated.

It has thus been shown that the results presented in Figure 6, while extending and improving the plots of Douglas and Churchill (25) and of McAdams (26), also serve as a powerful tool for determination of free-stream turbulence intensities.

Similar results for the front stagnation point heat transfer are presented in Figure 7 in the form of $(N_{Nu})_{D,r,s}/N_{Pr}^{0.4}$ vs. $K_s(N_{Re})_{D,r,\infty}$ where $K_s = 1 + \sqrt{D/W}$. The lower line labeled *0-1 percent turbulence intensity* represents the analytical laminar heat transfer level of Squire (24) described by the equation

$$\frac{(N_{Nu})_{D,r,s}}{(N_{Pr})^{0.4}} = 1.14\,[K_s(N_{Re})_{D,r,\infty}]^{1/2} \qquad (4)$$

Equation (4) is shown to be supported by the zero blockage and zero turbulence data of Schmidt and Wenner (14), the 0.9% turbulence intensity data ($D/W = 0.108$) of Zapp (9), the 0.6 to 0.9% turbulence intensity data ($D/W = 0.19$) of Kestin et al. (8), and two of the zero blockage data points of Giedt (15). The 3% turbulence intensity line drawn through corresponding data points of Zapp again indicates agreement with four of the data points of Giedt (15) as was the case in Figure 6. However, it falls below the 1.7 to 2.7 percent turbulence intensity data of Kestin et al. (not shown in Figure 7). Kestin et al. (8) do not consider their measurements to be of sufficient precision for quantitative conclusions. Thus, no further explanation for the above discrepancy is necessary.

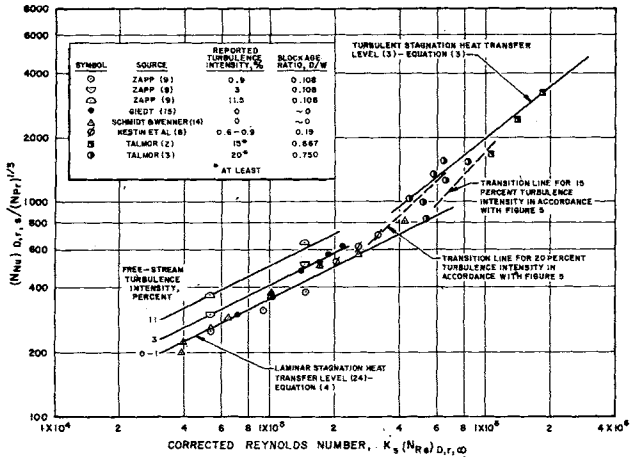

Fig. 7. Correlation of immersed cylinder front stagnation point heat transfer coefficients at high Reynolds numbers and a wide range of blockage ratios and turbulence intensities.

Stagnation point heat transfer data with combustion-induced turbulence present are given on the right-hand side of Figure 7. The upper line passing through these data represents the turbulent stagnation heat transfer level corresponding to Equation (3). It has been shown (2) that when the immersed cylinder boundary layer is turbulent essentially at stagnation (heat transfer coefficients increasing with distance from stagnation), the front stagnation heat transfer coefficient is identical to the average heat transfer coefficient around the cylinder. Thus, the same turbulent heat transfer equation describes both the front stagnation and average heat transfer results (2, 3).

Either one of Figures 6 and 7 can be used for determination of turbulence intensities, depending upon the nature of the heat transfer measurements taken (average or local at stagnation). Generally, average heat transfer measurements are easier to obtain, since they may consist of flowing water through an immersed cylinder and recording the water temperature rise across it. In fact, an immersed cylinder rig could be standardized for determining the combustion-induced turbulence intensity of the various propellant combinations.

Figures 6 and 7 do not reflect a possible effect of the scale of turbulence on immersed cylinder heat transfer. Such an effect was found to be significant at low cylinder Reynolds numbers where a Karman vortex street or a Strouhal effect is present (27). At high Reynolds numbers (Figures 6 and 7), where the Strouhal number is constant (24), the effect of turbulence scale is expected to be relatively minor, so that the turbulence intensity can be used as the main parameter of free-stream turbulence (6).

CONCLUSIONS

Transitional immersed cylinder heat transfer measurements constitute a powerful tool for determining free-stream turbulence intensities wherever direct measurements of turbulence intensity are not possible, for example, high-temperature combustors. By using this technique, the combustion-induced turbulence intensity of the nitrogen tetroxide–50% unsymmetrical dimethyl hydrazine–50% hydrazine propellants combination is at least 15 to 20%, depending on distance along the convergence section of the combustion chamber. Indications are that the turbulence intensity increases with gas acceleration.

An improved and extended correlation of immersed cylinder average and stagnation point heat transfer results is obtained through the determination of the turbulence level for high blockage data (2, 3) and the proper correction for channel blockage effects for all data compared (2, 3, 6, 8, 9, 14 to 16). The channel blockage correction factors of Pope (22) and Robinson and Han (21) seem appropriate for the average and front stagnation heat transfer coefficients, respectively.

As indicated by the successful determination of combustion-induced turbulence intensities from corresponding measurements of heat transfer to immersed cylinders (2, 3), the transition theory of van Driest and Blumer (17) is applicable to conditions of high turbulence and high pressure gradients.

NOTATION

C_D = drag coefficient
D = O.D. of immersed cylinder
g_c = conversion factor in Newton's law of motion, equals 32.2 (ft.)(lb.$_m$)/(sec.^{2})(lb.$_f$)
K = channel blockage correction factor for approach velocity
N_{Ma} = Mach number
m = Falkner-Skan exponent ($u_e \sim x^m$)
N_{Nu} = Nusselt number
p = pressure
N_{Pr} = Prandtl number
N_{Re} = Reynolds number
T = temperature
Tr = free-stream turbulence intensity, percent, = $(u'/u)100$
u = velocity in the direction of flow
u' = root-mean-square velocity fluctuation
W = channel width normal to the longitudinal axis of the immersed cylinder
x = distance from the forward stagnation point

Greek Letters

δ = boundary-layer thickness
η_e = $(\delta/x)(x\,u_e\,\rho_e/\mu_e)^{1/2}$
μ = viscosity
ρ = density

Subscripts

aw = adiabatic wall
avg. = average around the immersed cylinder
D = based on the cylinder O.D.
e = local conditions along the outer edge of the boundary layer
o = properties at stagnation conditions
r = reference point within the boundary layer
s = forward stagnation point
t = at the onset of transition
w = wall
∞ = approach (velocity)

Superscript

* = corrected for channel blockage

LITERATURE CITED

1. Hersch, Martin, *ARS J.*, **31**, 39 (1961).
2. Talmor, Eliyahu, *Chem. Eng. Progr. Symposium Ser. No. 59*, **61**, 50 (1965).
3. ———, paper presented at A.I.Ch.E. San Francisco Meeting (May, 1965).
4. ———, *Proc. 3rd Intern. Heat Transfer Conf.*, **1**, 77, Chicago, Ill. (Aug., 1966).
5. Giedt, W. H., *J. Aeronaut. Sci.*, **18**, 725 (1951).
6. Kestin, J., and P. F. Maeder, *Natl. Advisory Comm. Aeronaut. Tech. Note 4018* (1957).
7. Seban, R. A., *J. Heat Transfer*, **82**, 101 (1960).
8. Kestin, J., P. F. Maeder, and H. H. Sogin, *Z. Angew. Math. Phys.*, **12**, 115 (1961).
9. Zapp, G. M., M.S. thesis, Oregon State Coll. (1950).
10. Sogin, H. H., and V. S. Subramanian, *J. Heat Transfer*, **83**, 483 (1961).

11. Fand, R. M., and P. Cheng, *Intern. J. Heat Mass Transfer*, **6**, 571 (1963).
12. Sutera, S. P., P. F. Maeder, and J. Kestin, *J. Fluid Mech.*, **16**, 497 (1963).
13. Perkins, H. C., Jr., and G. Leppert, *Intern. J. Heat Mass Transfer*, **7**, 143 (1964).
14. Schmidt, Ernst, and Karl Wenner, *Natl. Advisory Comm. Aeronaut. Tech. Mem. 1147* (1947).
15. Giedt, W. H., *Trans Am. Soc. Mech. Engrs.*, **71**, 375 (1949).
16. Nelson, D. A., and Eliyahu Talmor, unpublished work.
17. van Driest, E. R., and C. B. Blumer, *Am. Inst. Aeronaut. Astronaut. J.*, **1**, 1303 (1963).
18. Buyuktur, A. R., J. Kestin, and P. F. Maeder, *Intern. J. Heat Mass Transfer*, **7**, 1175, (1964).
19. Thomas, D. G., *A.I.Ch.E. J.*, **11**, No. 3, 520 (1965).
20. Gazley, Carl, Jr., *J. Aerospace Sci.*, **20**, 19 (1953).
21. Robinson, W., and L. S. Han, *Proc. 2nd Conf. Midwest, Conf. Fluid Mech.*, Ohio State Univ., 349 (1952).
22. Pope, A., "Wind Tunnel Testing," 2 ed., Wiley, New York (1954).
23. Knudsen, J. G., and D. L. Katz, "Fluid Dynamics and Heat Transfer," McGraw-Hill, New York (1958).
24. Schlichting, Hermann, "Boundary Layer Theory," McGraw-Hill, New York (1960).
25. Douglas, W. J. M., and S. W. Churchill, *Chem. Eng. Progr. Symposium Ser. No. 18*, **52**, 23 (1956).
26. McAdams, W. H., "Heat Transmission," McGraw-Hill, New York (1954).
27. Van der Hegge Zijnen, B. G., *Appl. Sci. Res.*, **A7**, 205 (1958).

Manuscript received January 24, 1966; revision received April 25, 1966; paper accepted April 27, 1966.

Adsorption of Hydrocarbon Gas Mixtures at High Pressure

J. PRESTON MASON and C. E. COOKE, JR.

Esso Production Research Company, Houston, Texas

An experimental investigation was made of the adsorption on silica gel of components from light hydrocarbon mixtures, and the results were used to test a multicomponent adsorption theory. Experimental methods included a volumetric technique to measure pure component adsorption and flow techniques for adsorption from mixtures. Although the majority of measurements was made at 100°F., two mixtures were studied over the temperature range 40° to 160°F. Pressure was varied up to 1,800 lb./sq.in.abs. The Brunauer-Emmett-Teller (BET) theory of adsorption, as extended to mixtures by Hill, was tested against the experimental data and was found to be adequate for calculating adsorption from hydrocarbon mixtures of components heavier than methane. To account for nonideal behavior, the fugacity of each component in the gas and in the adsorbed phases was calculated by using the Benedict-Webb-Rubin equation of state. The differences in experimental and theoretical values for adsorption capacity were less than 10% for most of the conditions tested, but ranged up to about 25% for the highest pressures studied. Although the BET theory represents a simplified model of a complex process, it can be used to supply adsorption data for engineering application over ranges of pressure, temperature, and gas composition usually encountered in adsorption processing of natural gas mixtures.

The increasing use of adsorption separation techniques in the natural gas industry generates a need for basic data essential to effective design of adsorption processing equipment. Gas streams processed in adsorption plants usually contain about 90% or more of methane, with the remainder consisting of higher molecular weight paraffin hydrocarbons. Pressures commonly range from 300 to 1,200 lb./sq.in.abs. and temperatures from 80° to 120°F. Equilibrium adsorption capacities of commonly used adsorbents for the individual components of these complex, high-pressure, natural gas systems are therefore needed for a wide range of conditions.

Literature references to adsorption data for multicomponent natural gas mixtures are very scarce. Lewis et al. (*1*) and Gilmer and Kobayashi (*2*) published the only available information on adsorption of hydrocarbon gas mixtures on silica gel at pressures greater than atmospheric. However, all these results are limited to data for five binary mixtures. Most of the measurements were made at pressures less than those usually encountered in the field.

The investigation described in this paper was designed to supply experimental data concerning the adsorption capacity of individual components from natural gas mixtures on silica gel, one of the most commonly used adsorbents in the natural gas industry. Effects of pressure, gas composition, and, to a lesser extent, temperature were investigated over ranges encompassing those usually encountered in natural gas treating. Applicability of various adsorption theories to the resulting data was also investigated.

In the succeeding paragraphs, results of the adsorption capacity experiments are presented, and a multicomponent adsorption theory, capable of reproducing the experimen-